

**DOKUZ EYLUL UNIVERSITY**  
**GRADUATE SCHOOL OF NATURAL AND APPLIED SCIENCES**

**NUMERICAL STUDY ON THERMAL  
PERFORMANCE OF A NANOFLUID BASED FLAT  
PLATE SOLAR COLLECTOR**

by  
**Alper Mete GENÇ**

**December, 2017**

**İZMİR**

**NUMERICAL STUDY ON THERMAL  
PERFORMANCE OF A NANOFUID BASED  
FLAT PLATE SOLAR COLLECTOR**

**A Thesis Submitted to the  
Graduate School of Natural and Applied Sciences of Dokuz Eylul University  
In Partial Fulfillment of the Requirements for Degree of Master of Science in  
Mechanical Engineering, Energy Program**

**by  
Alper Mete GENÇ**

**December, 2017**

**İZMİR**

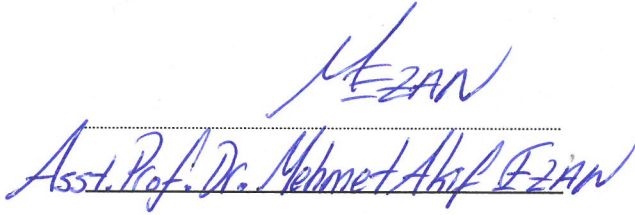
**M.Sc THESIS EXAMINATION RESULT FORM**

We have read the thesis entitled “NUMERICAL STUDY ON THERMAL PERFORMANCE OF A NANOFLUID BASED FLAT PLATE SOLAR COLLECTOR” completed by ALPER METE GENÇ under supervision of ASSOC. PROF. DR. ALPASLAN TURGUT and we certify that in our opinion it is fully adequate, in scope and in quality, as a thesis for the degree of Master of Science.

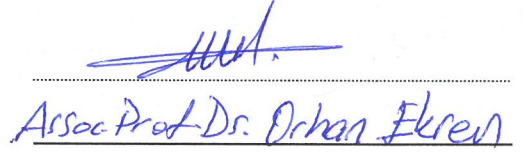


Assoc. Prof. Dr. Alpaslan TURGUT

Supervisor



(Jury Member)



(Jury Member)



Prof. Dr. Kadriye ERTEKİN

Director

Graduate School of Natural and Applied Sciences

## ACKNOWLEDGMENTS

I owe my deepest gratitude to my supervisor, Assoc. Prof. Dr. Alpaslan TURGUT for his patient supervision, inestimable, guidance and everlasting support throughout my graduate education. Studying with him was a privilege and helped me to decide to pursue an academic career. He taught me how to approach problems from a scientific point of view. I truly appreciate his encouragement and belief in me.

I would like also to express my special thanks to Asst. Prof. Dr. Mehmet Akif EZAN whose invaluable recommendations, expertise, understanding, and patience, improved considerably my research experience. Despite of his busy schedule, he provided a great effort and assigned a great deal of time for our constructive discussions. I am very grateful that I had the chance to work with him.

I want to express my sincere appreciation to Res. Asst. Serkan DOĞANAY, Halil Doğacan KOCA, Res. Asst. Tuba EVGİN and Alim ZORLUOL for helping me at every stage of my academic life. I appreciate their kind and perfectionist attitude, as well as their attention on my experiments.

I wish to express my special thanks to Yasemin ÇETİNTAŞ, İsmail Emre KALKAR and Nail Can KAYA for their contributions and great help.

Finally and most importantly, I would show my best thank to my family for their unlimited support in my whole life.

Alper Mete GENÇ

# NUMERICAL STUDY ON THERMAL PERFORMANCE OF A NANOFUID BASED FLAT PLATE SOLAR COLLECTOR

## ABSTRACT

Flat plate solar collectors (FPSCs) are commonly used devices to convert solar radiation into useful heat for a variety of thermal applications. Due to the lower thermal efficiencies of these systems, recently, nanofluids are suggested to be used in FPSCs as the working fluid to enhance their energy harvesting potential. This study introduces a transient heat transfer approach for determining the thermal inertia of each component such as glass, trapped air, absorber and working fluid for nanofluid based flat plate solar collectors. The analyses were carried out with water and three different volumetric concentrations of alumina nanoparticles as 1, 2 and 3 volumetric percent. Mass flow rate of the heat transfer fluid is varied in a wide range, between 0.004 and 0.06 kg/s, to demonstrate the effect of thermophysical properties at different flow Reynolds numbers. The results demonstrate that outlet temperature of the FPSCs increases with increasing particle concentration. Moreover, the outlet temperature decreases with increasing mass flow rates. On the other hand, thermal efficiency of the FPSCs increases with increasing mass flow rates regardless of the type of heat transfer fluids. However, nanofluids can increase the thermal efficiency of the FPSCs at lower mass flow rates and the thermal efficiency increases with increasing particle concentration. Beyond a critical mass flow rate the base fluid becomes effective working fluid and the thermal efficiency decreases with increasing particle concentration. For the current study, the critical mass flow rate is determined to be 0.016 kg/s.

**Keywords:** Flat-plate, solar collector, transient analysis, alumina, nanofluids

# NANOAKIŞKAN BAZLI DÜZLEMSEL GÜNEŞ TOPLAYICININ ISIL PERFORMANSININ SAYISAL ANALİZİ

## ÖZ

Düzlemsel tip güneş toplayıcılar, güneş ışınımını, çeşitli ısı uygulamalarda kullanılır ısıya dönüştürmek için yaygın olarak kullanılan cihazlardır. Bu tip cihazların düşük ısı verim değerlerine sahip olması nedeniyle, enerji toplama potansiyellerini artırmak için iş akışkanını olarak nanoakışkanların kullanılması önerilmektedir. Bu çalışmada, nanoakışkan kullanılan düzlemsel güneş toplayıcının koruyucu cam, hava, yutucu ve iş akışkanından oluşan her bir bileşenin ısı ataletlerinin belirlenmesi amacıyla geçici rejim ısı transfer yaklaşımı uygulanmıştır. Analizler, temel akışkan olarak kullanılan su ile birlikte, yüzde 1, 2 ve 3 hacimsel konsantrasyonlarda alümina nano parçacıklarına sahip nanoakışkanlar için gerçekleştirilmiştir. Farklı Reynolds sayılarındaki termofiziksel özelliklerin etkisinin gösterilmesi amacıyla, ısı transfer akışkanlarının kütle debileri 0,004 ve 0,06 kg/s aralığında seçilmiştir. Sonuçlar, toplayıcı çıkış sıcaklığının artan parçacık konsantrasyonu ile arttığını göstermektedir. Ek olarak, çıkış sıcaklığı, artan kütle debisiyle beraber azalmaktadır. Diğer yandan, toplayıcının ısı verimi ısı transfer akışkanının türüne bakılmaksızın artan kütle debisiyle beraber artmaktadır. Fakat nanoakışkanlar, toplayıcı ısı verimini sadece düşük kütle debilerinde artırmakta ve parçacık konsantrasyonu artışıyla beraber ısı verim artmaktadır. Kritik kütle debisinden daha yüksek kütle debilerinde temel akışkan daha etkili olmakta ve ısı verim artan parçacık konsantrasyonu ile beraber azalmaktadır. Sunulan bu çalışmada, kritik kütle debisi 0,016 kg/s olarak belirlenmiştir.

**Anahtar Kelimeler:** Düzlemsel, güneş toplayıcı, geçici rejim analizi, alümina, nanoakışkanlar

## CONTENTS

	<b>Page</b>
M.Sc THESIS EXAMINATION RESULT FORM.....	ii
ACKNOWLEDGMENTS .....	iii
ABSTRACT .....	iv
ÖZ .....	v
LIST OF FIGURES .....	vii
LIST OF TABLES .....	ix
<b>CHAPTER ONE - INTRODUCTION .....</b>	<b>1</b>
<b>CHAPTER TWO - MATERIAL AND METHOD .....</b>	<b>7</b>
2.1. Definition of the Problem.....	7
2.2. Numerical Model.....	8
2.3. Data Reduction .....	11
2.4. Solution Method & Validation .....	13
<b>CHAPTER THREE - RESULTS AND DISCUSSIONS .....</b>	<b>16</b>
3.1. Effect of Weather Conditions on the Outlet Temperature .....	16
3.2. Effect of Working Fluid & Mass Flow Rate on the First Law Efficiency .....	18
3.3. Effect of Working Fluid & Mass Flow Rate on the Outlet Temperature .....	23
<b>CHAPTER FOUR - CONCLUSION .....</b>	<b>27</b>
<b>REFERENCES .....</b>	<b>29</b>
<b>APPENDICES .....</b>	<b>35</b>

## LIST OF FIGURES

	<b>Page</b>
Figure 1.1 Conversion of solar energy into other forms of energy .....	2
Figure 1.2 A typical view of flat plate solar collector.....	3
Figure 2.1 Mathematical Model.....	8
Figure 2.2 Time dependent incident solar radiation and ambient temperature variations for representative months.....	12
Figure 2.3 Time-wise variation of the outlet temperature.....	14
Figure 2.4 The variation of daily solar radiation and the outlet temperature of the FPSC.....	15
Figure 3.1 Influence of climatic conditions on the FPSC outlet temperature and useful heat for 1% Al <sub>2</sub> O <sub>3</sub> -water nanofluid at 0.03 kg/s.....	17
Figure 3.2 Daily average thermal efficiency of the FPSC for various mass flow rates in October .....	19
Figure 3.3 Daily average thermal efficiency of the FPSC for various HTFs.....	20
Figure 3.4 Collector efficiency as a function of $(T_{in} - T_{\infty})/I_{solar}$ parameter for water – Influence of mass flow rate .....	22
Figure 3.5 Collector efficiency as a function of $(T_{in} - T_{\infty})/I_{solar}$ parameter – Influence of the type of HTF .....	22
Figure 3.6 Effect of the mass flow rate of the HTF on the instantaneous outlet temperature for (a) January and (b) July .....	24
Figure 3.7 The effect of mass flow rates on the average outlet temperature .....	26
Figure 3.8 Daily average outlet temperature of the FPSC under various HTFs .....	26



## LIST OF TABLES

	<b>Page</b>
Table 2.1 Collector parameters .....	8
Table 2.2 Thermophysical properties of the FPSC components.....	10
Table 2.3 Physical characteristics of the working fluids.....	11



## **CHAPTER ONE**

### **INTRODUCTION**

Energy is an essential factor for the development and economic growth of the countries. Over the past decades, energy consumption has increased significantly due to improvement in life's quality and industrialization progress (Leong et al., 2016). In order to consider the increasing energy demand of the world, various energy agencies such as: International Energy Agency (IEA, 2016), International Energy Outlook (IEO, 2017) and The Institute of Energy Economics-Japan (IEEJ, 2016) have been presenting long-term energy projections. These projections provide what may happen given certain assumptions under different scenarios. According to the main scenario of International Energy Agency (IEA, 2016), it is expected that global energy demand will grow 30% by 2040. Today, almost 86% of the primary energy consumption is met by fossil fuels (BP, 2016). However, fossil fuels are limited sources and also have negative effects on global warming. As released by European Commission (UNFCCC, 2015) according to the Paris Climate Agreement, "Governments agreed on a long-term goal of keeping the increase in global average temperature to well below 2°C above pre-industrial levels and to aim to limit the increase to 1.5°C". The agreement has suggested shifting the resources away from polluting fossil fuels to clean energy and therefore, renewable energy has gained more important role since it is clean, safe and sustainable. As a promising renewable energy source, solar energy has attracted considerable attention in recent years. The conversion of solar energy into different other forms such as thermal energy, electrical energy, mechanical energy and chemical energy is shown in Figure 1.1 (Suman, Khan & Pathak, 2015). The power from the sun intercepted by the earth is approximately  $1.8 \times 10^{11}$  MW and about 30% of this reaches the earth. At every 20 min, the sun produces enough power to meet the requirements of the world for an entire year (Hussein, 2016).

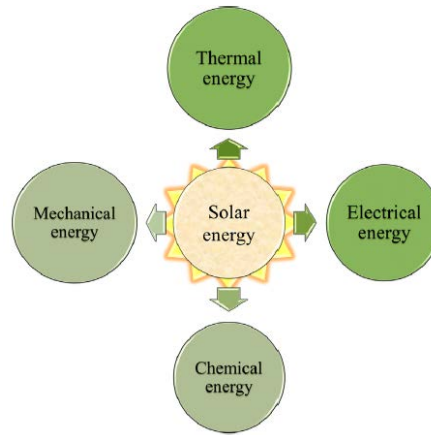


Figure 1.1 Conversion of solar energy into other forms of energy (Suman, Khan & Pathak, 2015)

Among the several devices for harvesting solar energy, solar collectors are the most popular ones to convert solar radiation into useful heat. Kalogirou (2004) presented an exhaustive review on different types of solar thermal collectors and their applications. Although the most commonly used solar collectors are flat plate types, they have comparatively lower efficiencies and outlet temperatures (Yousefi, Veisy, Shojaeizadeh & Zinadini, 2012). A typical flat plate solar collector is shown in Figure 1.2. Suman et al. (2015) recently reviewed the advancements in solar technology by focusing on the methodologies of enhancing their thermal performance. A suggestion has been made to replace the heat transfer fluid (HTF) by new generation working fluids such as nanofluids. Nanofluids are composed of higher thermal conductive nanoparticles such as metal oxide, metal or carbon that are dispersed within conventional base fluids such as water, oil, ethylene glycol or brines. Therefore, nanofluids that are used in thermal applications to transfer thermal energy may be called as nano-enhanced heat transfer fluids (ne-HTFs). Although Masuda, Ebata & Teramae (1993) were the first who showed the great potential of improving the thermal conductivity of fluids by adding conductive nanoparticles, the nanofluid term was named by Choi (1995). Since then, many researchers have studied different properties and possible applications of nanofluids. One can find valuable information on the subject in the recent review papers. Ganvir, Walke & Kriplani (2016) presented a comprehensive review of heat transfer characteristics of nanofluids. They mentioned that the further application oriented research of nanofluid is the need of an hour. In addition, they concluded that nanofluid with enhanced thermal conductivity brings about enhanced heat transfer. Devenviran & Amirtham (2016) described the heat

transfer potential of different types of nanofluids. They mentioned that further research on various applications of nanofluids should be carried out. It was also mentioned that the requirement to improve the efficiency of thermal systems relies highly on the enhancement of thermal conductivity of the working fluid. Raja, Vijayan, Dineshkumar & Venkatesan (2016) published a review paper on characteristics, heat transfer performances and applications of nanofluids. It is noted that convective heat transfer behavior of nanofluids is superior to conventional fluids.

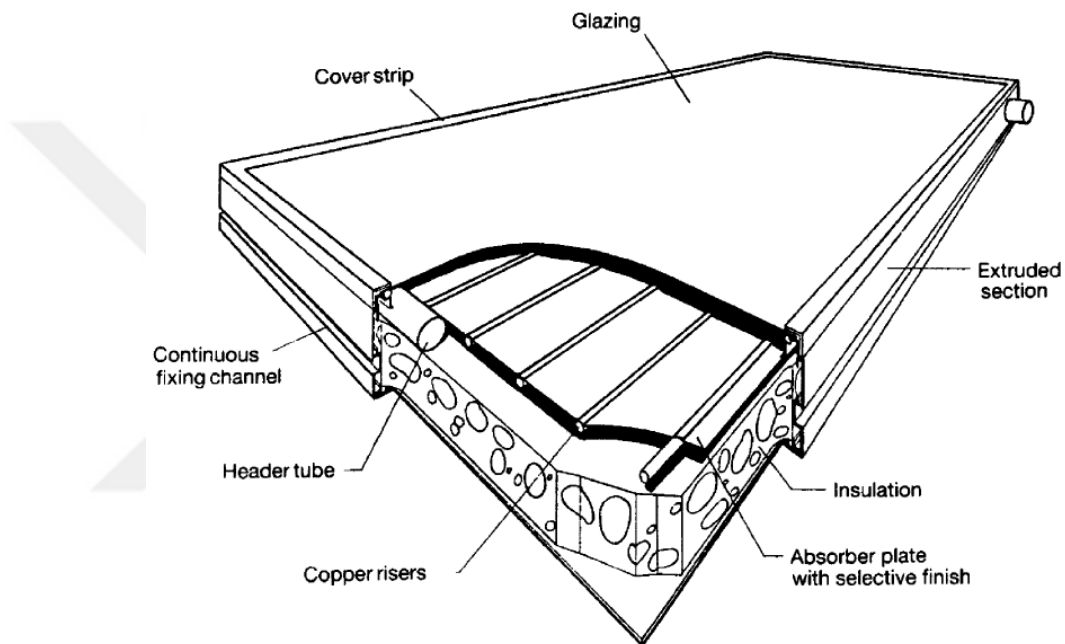


Figure 1.2 A typical view of flat plate solar collector (Kalogirou, 2004)

Regarding the existing literature on nanofluid based solar energy systems, there are several review reports. Pandey & Chaurasiya (2017) emphasized that using nanofluids on FPSCs bring about advantages such as cost effectiveness, being environmentally friendly and compact and lightweight. Verma & Tiwari (2015) reviewed the nanofluids' effectiveness on the efficiency of solar energy systems, mainly: solar collectors, photovoltaic systems, solar thermoelectric and energy storage system. They concluded that nanofluids can be a better solution for use as heat transfer fluids in solar thermal systems. Sarsam, Kazi & Badarudin (2015) reported a comprehensive review on nanofluid applications in flat plate solar collectors. They confirmed that nanofluids can be used effectively to enhance the performance of FPSCs.

Above mentioned reports present many experimental studies on nanofluid based FPSCs. In the most recent one, Verma, Tiwari & Chauhan (2017) investigated the effect of a wide variety of nanofluids on the performance of flat plate solar collector under steady state conditions. They concluded that the thermal efficiency was improved by 23.5% using MWCNTs/water at 0.75% (vol.). Verma, Tiwari & Chauhan (2016) experimentally investigated the effect of MgO/water nanofluid as working fluid on the flat plate solar collector. They found that the efficiency of solar collector was increased by using MgO/water nanofluid in comparison with water by 9.34% for 0.75% particle volume fraction and volume flow rate at 1.5 lpm. Vincely & Natarajan (2016) investigated the influence of graphene oxide nanofluid on the performance of flat plate solar collector for steady state conditions. They reported that thermal efficiency was enhanced by 7.3% at 2% (wt.) and 0.01167 kg/s mass flow rate. Colangelo et al. (2015) performed an investigation for a flat plate solar collector by using Al<sub>2</sub>O<sub>3</sub>/water nanofluid at a high volumetric concentration as 3%. The results show that the enhancement of thermal efficiency was up to 11.7% compared to water.

The experimental methods require both accurate test equipment and long experimentation time so that numerical methods could be a savior in proper circumstances. However, the numerical studies on nanofluid based FPSCs are limited in the literature. Faizal, Saidur, Mekhilef & Alim (2013) investigated the potential of various nanofluids such as; CuO/water, SiO<sub>2</sub>/water, TiO<sub>2</sub>/water and Al<sub>2</sub>O<sub>3</sub>/water to optimize the size of the collector for providing economic and environmental benefits. The conclusion is that the efficiency of FPSC has increased by 38.5% by using CuO nanofluids at 3% volume fraction. Tora & Moustafa (2013) developed a model to predict the heat transfer performance of Al<sub>2</sub>O<sub>3</sub>/water nanofluid on FPSC. They found that the thermal efficiency increases by 14.7% and 37.44% by incorporating 0.01% (vol.) and 0.5% (vol.) of nanoparticles into the base fluid, respectively. Nasrin & Alim (2014a) evaluated the heat transfer performance of different nanofluids on the FPSC. They demonstrated that the highest collector efficiency is found as 89% for Ag/water nanofluid at 5% (vol.). Nasrin & Alim (2014b) studied the effect of Al<sub>2</sub>O<sub>3</sub>/water nanofluid on FPSC. They concluded that collector efficiency was enhanced by increasing Reynolds number and decreasing Prandtl number. Ekramian, Etemad &

Haghshenasfard (2014) focused on developing a model to investigate the heat transfer performance of MWCNT/water, Al<sub>2</sub>O<sub>3</sub>/water and CuO/water nanofluids with mass concentrations of 1, 2 and 3% on FPSC. According to their results, CuO/water nanofluid shows a better performance on the thermal efficiency which increases by 20%.

The aforementioned numerical studies consider steady state heat transfer for the analyses. However, climatic conditions such as solar irradiation and ambient temperature are not very suitable for steady-state analyses. For being able to predict the time-dependent behavior of the collector under variable solar irradiation and ambient temperature, one should use the transient conditions (Rodríguez-Hidalgo, Rodríguez-Aumente, Lecuona, Gutiérrez-Urueta & Ventas, 2011). Moreover, since each component of the solar collector, i.e. the working fluid, absorber, trapped air and glass, has thermal inertia (or *thermal capacitance*), the transient experimental and/or numerical methods are the only way to capture the real thermal response of the solar unit. Rodríguez-Hidalgo et al. (2011) stated that the transient heat transfer model is the most accurate way to predict the thermal inertia since the model can provide the instantaneous heat production from the FPSC. Such a transient output is useful if the solar collector is implemented in a multi-generation system such as an absorption cooling Osório & Carvalho (2014) or thermal energy storage (TES) unit (Fernandes, Brites, Costa, Gaspar & Costa, 2016). Several numerical studies about the transient behavior of the flat plate solar collectors, using water as the working fluid, can be found in the literature. Amer, Nayak & Sharma (1998) developed a transient numerical model to characterize the dynamic behaviour of FPSCs. Nayak, Amer & Deshpande (2000) presented the comparison of nine different transient test methods for FPSCs. Kong et al. (2012) developed a transfer function method, in order to accurately and robustly estimate FPSC parameters and predict the thermal performance of FPSC under dynamic test conditions. Hamed, Fella & Brahim (2014) emphasized that the study of the transient response of FPSCs attracts significant attention due to the innovative dynamic test methods for evaluating and predicting their thermal performance precisely.

As referred above, transient methods provide a means to estimate the thermal performance of solar collectors much better. Moreover, it is mentioned in the literature that nanofluids increase the thermal performance of FPSCs. To get a better achievement in real solar application systems that works with nanofluids, numerical transient analyses would be more beneficial. However, to the best of authors' knowledge, there is no study so far on numerical transient analyses of nanofluid based FPSCs. Therefore, this numerical study aims to investigate the transient behavior of  $\text{Al}_2\text{O}_3$ -water nanofluid based FPSC for different particle volumetric concentrations and mass flow rates at different climatic conditions and to compare with water.  $\text{Al}_2\text{O}_3$ -water nanofluid is selected due to its well-known thermophysical properties (Turgut, Saglanmak & Doganay, 2016) and thermal performance (Turgut & Doganay, 2014; Doganay & Turgut; 2015) based on the authors' previous experimentations.

The thesis divided into four chapters. In chapter one a short introduction to solar energy, flat plate solar collectors and nanofluids are given. In addition, nanofluid based flat plate solar collectors and numerical studies are also given. Moreover, the objectives of this research are presented. In chapter two, developed mathematical model, properties of the materials of working fluids are demonstrated. Our numerical results for outlet temperature and thermal efficiency of the flat plate solar collector are given in chapter three. In chapter four, the concluding remarks are summarized and future works are recommended for nanofluid based solar collectors.

## **CHAPTER TWO**

### **MATERIAL AND METHOD**

In the current work, a two-dimensional and transient FPSC model is numerically investigated. The schematic and the boundary conditions of the problem is presented in Figure 2.1.

#### **2.1. Definition of the Problem**

The flat plate solar collector is composed of following five major components:

- A transparent glass cover with 3.2 mm thickness is used for reducing both radiative and convective heat losses from the selective surface.
- Trapped air is transparent, which prevents the radiative heat loss from the absorber surface through the ambient.
- The absorber is covered with a copper sheet, and its surface has been painted by dark color for high absorption so that the surface acts as selective.
- Copper tubes are placed under the copper sheet to circulate the fluid where the useful heat is transferred from the absorber to the working fluid.
- Heat transfer fluid (HTF) is used to extract heat from the absorber surface.

The design parameters of the solar collector are taken from Hamed et al. (2014) and are listed in Table 2.1. To reduce the 3D coupled heat transfer and the fluid flow problem into a simplified 2D transient mathematical model, the following assumptions have been considered;

- Losses by radiation and convection from the bottom and side surfaces of the insulation are negligible,
- The convective heat transfer coefficient that arises from the natural convection of trapped air between the transparent cover and the absorber is identical for the top and bottom surfaces of the enclosure and is uniform along the flow direction.
- The sky is regarded as a blackbody.



- The transparent cover is opaque to infrared radiation. The physical properties of materials are assumed to be independent of the temperature variations.

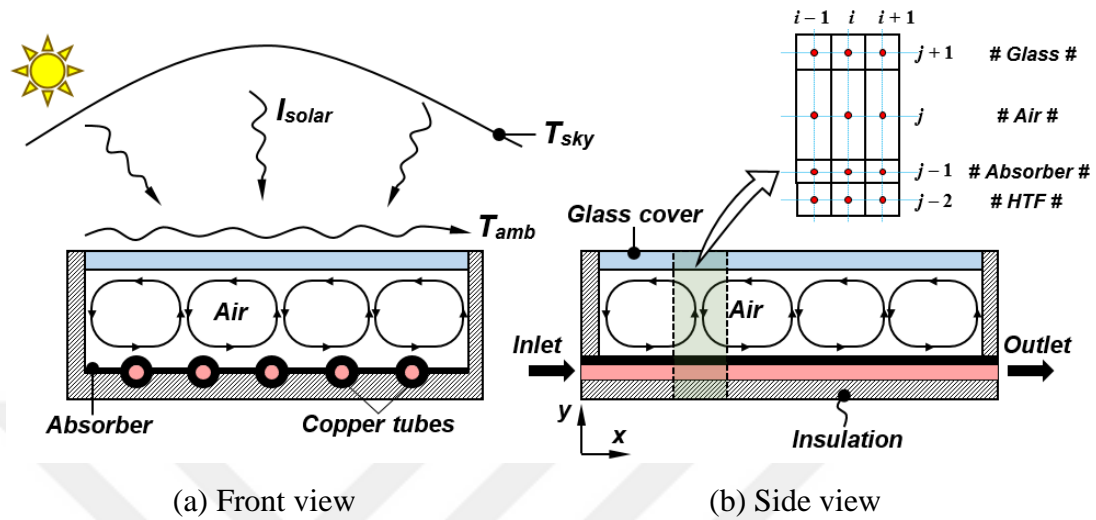


Figure 2.1 Mathematical Model

Table 2.1 Collector parameters (Hamed, Fellah & Brahim, 2014)

<b>Dimensions</b>	1941 x 1027 x 88 (mm)
<b>Transparent cover</b>	<i>Glass</i> Thickness: 3.2 mm Transmissivity ( $\tau$ ): 0.9 Emissivity ( $\epsilon$ ): 0.89
<b>Absorber</b>	<i>Copper</i> Thickness: 1.8 mm Absorptivity ( $\alpha$ ): 0.95 Emissivity ( $\epsilon$ ): 0.05
<b>Tubes</b>	<i>Copper</i> Diameter: 8.81 mm

## 2.2. Numerical Model

A two-dimensional mathematical model for a FPSC is developed in MATLAB by using the finite difference approach. Energy balance equations are written for each component of the FPSC, and an iterative solution procedure is followed to resolve the resultant set of linear equations. On the external surface of the glass cover, only a portion of the incident solar radiation could be transferred to the working fluid through

the absorber plate due to the convective and radiative heat losses towards the ambient and sky, respectively. Following the reductions that are listed in the previous section, the overall energy balance of a unit control volume within the glass cover can be written as,

$$\left( mc \frac{\partial T}{\partial t} \right)_g = \left( kA_c \frac{\partial T}{\partial x} \right)_g + I_{solar} \tau_g \alpha_g A_s - h_{\infty} A_s (T_g - T_{\infty}) - \varepsilon_g \sigma A_s (T_g^4 - T_{sky}^4) + \varepsilon_{abs} \sigma A_s (T_{abs}^4 - T_g^4) - h_{air} A_s (T_g - T_{air}) \quad (2.1)$$

where  $h_{\infty}$  and  $h_{air}$  indicate the convective heat transfer coefficients on the external and the inner surfaces of the glass cover, respectively. The incident solar radiation ( $I_{solar}$ ) and ambient temperature ( $T_{\infty}$ ) are defined according to the transient meteorological data of Izmir City, Turkey (PVGIS, 2017). To introduce the influence of heat transfer fluid on the performance of the FPSC on a yearly basis, the analyses are conducted for four selected representative months, January, April, July, and October. For these representative months, the time dependent incident solar radiation and ambient temperature variations are shown in Figure 2.2. The following equation is implemented to evaluate the convective heat transfer coefficient on the external surface of the glass as a function the wind speed (Duffie & Beckman, 1974),

$$h_{\infty} = 3.9v_{wind} + 5.62 \quad (2.2)$$

where the wind speed,  $v_{wind}$ , is defined as 3 m/s for Izmir city, Turkey (MGM, 2017). According to Swinbank's formula (Swinbank, 1963), the sky temperature is defined as follows,

$$T_{sky} = 0.0552T_{\infty}^{1.5} \quad (2.3)$$

The energy balance equation for a unit control volume of the trapped air between the glass cover and absorber is expressed as:

$$\left( mc \frac{\partial T}{\partial t} \right)_{air} = \left( kA_c \frac{\partial T}{\partial x} \right)_{air} + h_{air} A_s (T_g - T_{air}) + h_{air} A_s (T_{abs} - T_{air}) \quad (2.4)$$

where  $h_{air}$  represents the convective heat transfer coefficient that corresponds to the natural convection of trapped air between the cover glass and absorber plate. Duffie & Beckman (1974) suggest the following empirical correlation to evaluate  $h_{air}$ ,

$$Nu_{air} = [0.06 - 0.017(\theta / 90)]Gr^{1/3} \quad (2.5)$$

where  $\theta$  is the angle of inclination of the collector. As suggested by Panayiotou et al. (2016), the angle of inclination is defined as  $\theta = 45^\circ$ . On the other hand, the definition of dimensionless Gr number is given in the nomenclature. For the absorber, the energy balance equation of a unit control volume can be written as follows:

$$\left( mc \frac{\partial T}{\partial t} \right)_{abs} = \left( kA_c \frac{\partial T}{\partial x} \right)_{abs} + I_{solar} \tau_{abs} \alpha_{abs} A_s - h_{htf} A_s (T_{abs} - T_{htf}) + \varepsilon \sigma A_s (T_g^4 - T_{abs}^4) - h_{air} A_s (T_{abs} - T_{air}) \quad (2.6)$$

For the fluid inside the riser tubes, energy equation of a unit control volume is given by:

$$\left( mc \frac{\partial T}{\partial t} \right)_{htf} = \left( kA_c \frac{\partial T}{\partial x} \right)_{htf} + h_{htf} A_s (T_{htf} - T_{abs}) \quad (2.7)$$

where the convective heat transfer coefficient of HTF is obtained by using the well-known Dittus-Boelter correlation (Incropera, Dewitt, Bergman & Lavine, 2006). The thermophysical properties of glass, air, and the absorber plate are listed in Table 2.2.

Table 2.2 Thermophysical properties of the FPSC components (Incropera, Dewitt, Bergman & Lavine, 2006)

<b>Material</b>	<b>Specific Heat, <math>c</math></b> (J/kgK)	<b>Density, <math>\rho</math></b> (kg/m <sup>3</sup> )	<b>Thermal Conductivity, <math>k</math></b> (W/mK)
Glass	750	2500	1.4
Air	1007	1.614	0.03
Absorber	385	8933	401

A total of three water-based ne-HTFs are considered in the current work. The specific heat and density values of ne-HTFs are obtained by using the following equations depending on classical mixture rules (Eastman, Phillpot, Choi & Keblinski, 2004),

$$c_{nf} = \frac{\phi_p (\rho c)_p + (1 - \phi_p)(\rho c)_f}{(1 - \phi_p)\rho_f + \phi_p\rho_p} \quad (2.8)$$

$$\rho_{nf} = (1 - \phi_p)\rho_f + \phi_p\rho_p \quad (2.9)$$

where  $\rho_f$  and  $\rho_p$  are the base fluid density and particle density, respectively.  $\phi_p$  is the volume fraction of the nanofluid. Besides, instead of implementing the theoretical models to evaluate the viscosity and thermal conductivity of the working fluids, these two properties are defined regarding the experimental measurements of Turgut et al. (2016). Distilled water is used as the based fluid and three different volume fractions of Al<sub>2</sub>O<sub>3</sub>, such as 1%, 2%, and 3%, are used in the analysis. Thermophysical properties of the working fluids are shown in Table 2.3.

Table 2.3 Physical characteristics of the working fluids (Turgut, Saglanmak & Doganay, 2016)

Material	Specific Heat, $c$	Density, $\rho$	Thermal Conductivity, $k$	Viscosity, $\mu$	Pr
	(J/kgK)	(kg/m <sup>3</sup> )	(W/mK)	(mPas)	(-)
Water	4180	1000	0.576	1.00	7.26
Al <sub>2</sub> O <sub>3</sub> -H <sub>2</sub> O (1% vol.)	4060.8	1023.7	0.620	1.12	7.33
Al <sub>2</sub> O <sub>3</sub> -H <sub>2</sub> O (2% vol.)	3947.6	1050.8	0.634	1.28	7.94
Al <sub>2</sub> O <sub>3</sub> -H <sub>2</sub> O (3% vol.)	3839.9	1077.8	0.655	1.57	9.17

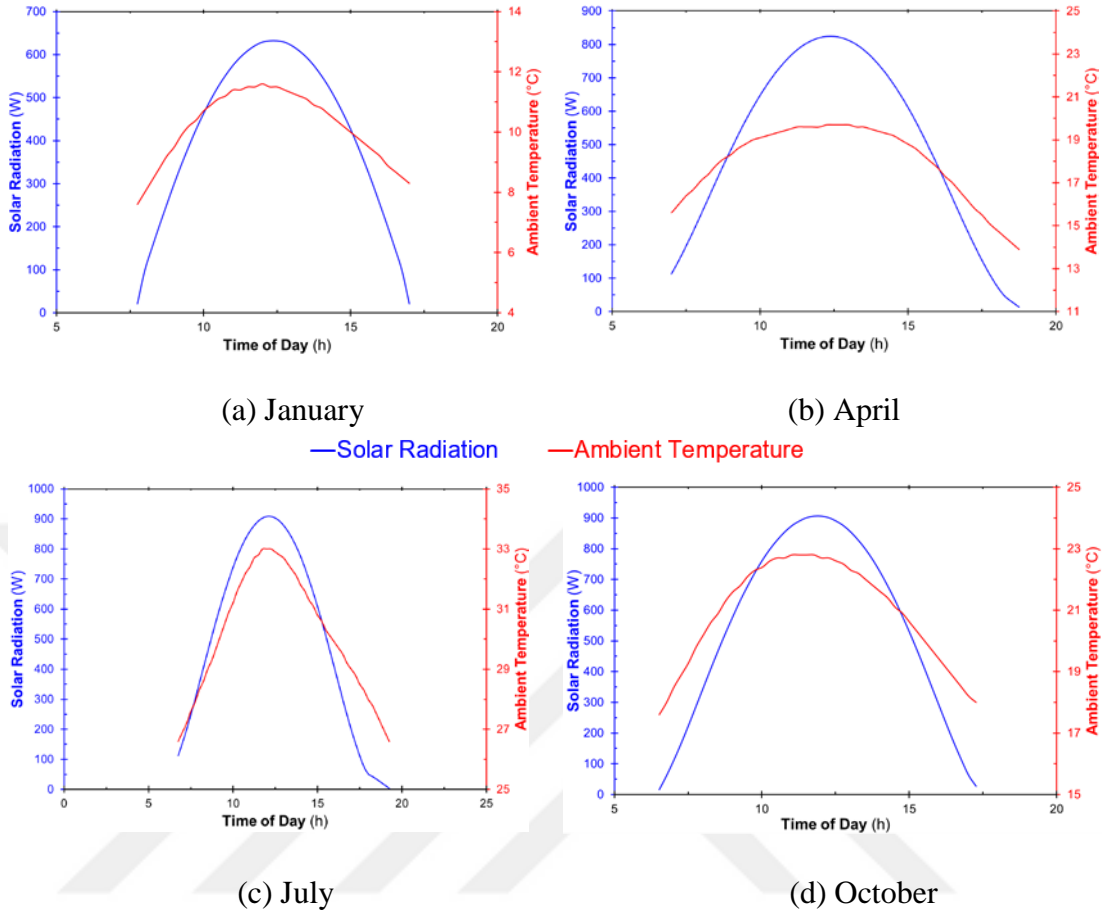


Figure 2.2 Time dependent incident solar radiation and ambient temperature variations for representative months

### 2.3. Data Reduction

The thermal efficiency of the flat plate solar collector can be calculated as:

$$\eta = \frac{q_{\text{useful}}}{I_{\text{solar}} A_s + \dot{W}_{\text{pump}}} = \frac{\dot{m}c(T_{\text{out}} - T_{\text{in}})}{I_{\text{solar}} A_s + \dot{W}_{\text{pump}}} \quad (2.10)$$

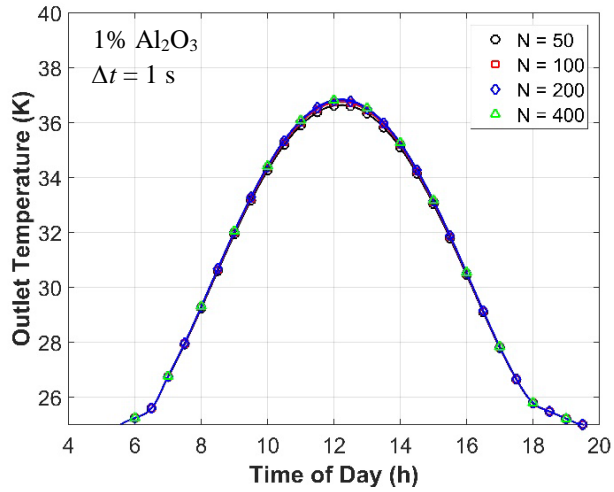
where the pumping power can be obtained from the following equation,

$$\dot{W}_{\text{pump}} = (\dot{m}/\rho)\Delta P \quad (2.11)$$

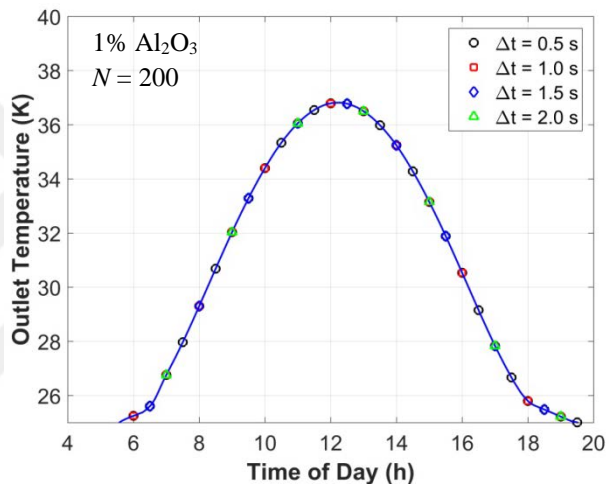
For a smooth straight tube, the pressure drop is evaluated from the energy balance across the inlet/outlet sections as  $\Delta P = f(L/V)(\rho V^2/2)$ . Where  $f$  stands for Darcy friction factor and is evaluated from the well-known Moody chart (Cengel, Turner, Cimbala & Kanoglu, 2005).

## 2.4. Solution Method & Validation

As shown in Figure 2.1, in the mathematical model, the FPSC is divided into four computational domains along the  $y$ -direction. Eqs. (1), (4), (6) and (7) correspond to the differential form of the energy equations for each component of the FPSC unit. The current form of the equations include both the time-wise and span-wise temperature variations. The differential energy equations are transformed into the algebraic sets of equations by using the finite difference method (Duffie & Beckman, 1974). The diffuse terms are discretized using the central differencing scheme and for the convective terms upwind scheme (Patankar, 1980) is applied. An implicit approach is proposed to resolve the transient terms. Gauss-Siedel iteration method (Panatkar, 1980) is applied to resolve the sets of equations. For each time step, the iterations are carried out to achieve the convergence criteria of  $10^{-7}$ . It is observed that the energy balance is satisfied for each time step with a maximum error of 0.01%. The numerical procedure is coded as a MATLAB script. To observe the influences of mesh intensity and the time step size on the predicted results, a set of preliminary analyses are conducted. The total number of mesh is varied from 50 to 400, and the time-step size is selected in the range of 0.5 s to 2 s. Figure 2.3 represents the comparative results for the outlet temperature of HTF in July for a constant flow rate of 0.03 kg/s. It is clear that the variation of total number mesh and/or time step-size do not cause any remarkable changes in the time-wise variation of the outlet temperature. The maximum deviation between the finest and the coarse mesh is found to be less than 0.1%. Besides, regarding the time-step size, the maximum difference is obtained as 0.05%. Consequently, the preliminary survey ensures that the results are independent of the number of mesh and the time-step size.



(a)



(b)

Figure 2.3 Time-wise variation of the outlet temperature (a) Effect of total number of mesh –  $\Delta t = 1$  s (b) Effect of time step size –  $N = 200$

The validity of the current code is proven by reproducing the transient numerical work of Onyegegbu & Morhenne (1993). In the FPSC model of Onyegegbu & Morhenne (1993), the collector dimensions and specific mass flow rate are given as  $L = 3\text{m}$ ,  $W = 0.06\text{ m}$  and  $G = 0.01\text{ kg/sm}^2$ . In Figure 2.4 the variation of daily solar radiation and the outlet temperature of the FPSC are shown. The maximum error is obtained approximately as 0.5% for the outlet temperature.

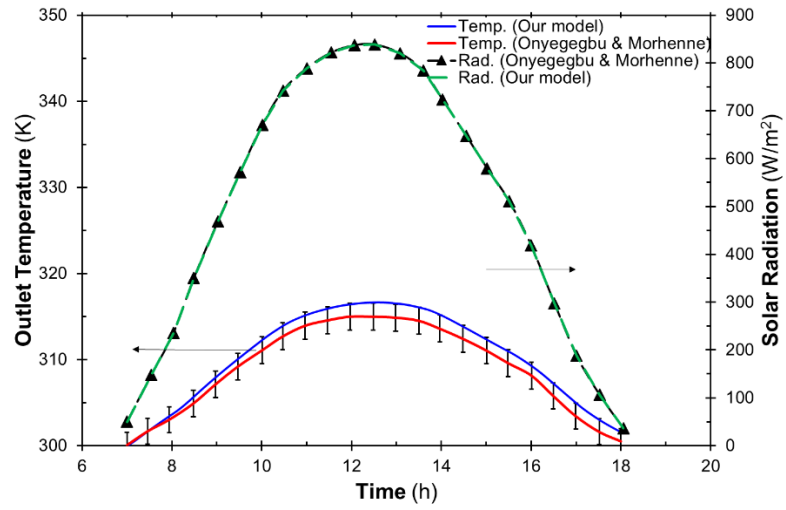


Figure 2.4 The variation of daily solar radiation and the outlet temperature of the FPSC



## **CHAPTER THREE**

### **RESULTS AND DISCUSSIONS**

In the analyses, four representative months, January, April, July and October, are chosen to evaluate the performance of the FPSC with ne-HTF. The transient solar irradiation and ambient temperature data are defined according to the monthly average daily weather data of Izmir City, Turkey (PVGIS, 2017). The inlet temperature of the working fluids to the FPSC is assumed to be constant throughout the day at 25°C (Hamed et al., 2014). Water is used as the base fluid. In addition to water, ne-HTFs are also considered with volume fractions of 1%, 2%, and 3%. As stated by Moghadam, Farzane-Gord, Sajadi & Hoseyn-Zadeh (2014), mass flow rate of the working fluid is one of the most important parameters which affects the performance of the flat plate solar collectors. Thus, the mass flow rate of the HTF is varied in a wide range, 0.004 to 0.06 kg/s, to introduce the influence of thermophysical properties at different Reynolds numbers.

#### **3.1. Effect of Weather Conditions on the Outlet Temperature**

Figure 3.1 demonstrates the time-wise variations of the incident solar radiation, the outlet temperature of the HTF and the useful heat for four selected months. The residue of the energy balance of the system at each time-step is also represented in the same figure. The maximum deviation, regarding the energy balance, is obtained less than 0.8% and it proves that the predicted results satisfy the first law of Thermodynamics in each time-step with a reasonable accuracy. In each case of Figure 3.1, representative of the mass flow rate of the HTF is defined to be 0.03 kg/s, which is a moderate flow rate for the current work, and the working fluid is water based nanofluid with 1% of Al<sub>2</sub>O<sub>3</sub> nanoparticles. It is obtained that the highest outlet temperature of the ne-HTF varies in the range of 32.9°C and 36.7°C for this preliminary survey. The mean outlet temperatures for spring, summer and fall seasons, which corresponds to April, July and October months, the outlet temperature of the HTF are also very close to each other. The difference is less than 1.5°C in terms of the average outlet temperatures. Besides, since the insolation periods are approximately 13 h, 14 h and 11 h for April,

July, and October, respectively, in July, the FPSC can satisfy the hot fluid demand for a longer period. In the current flow rate condition, the collector can provide the ne-HTF with an average temperature of 30°C throughout the year. That is, the system can only be used to supply domestic hot water for the current working conditions. The mass flow rate of the ne-HTF significantly affects the useful heat and the outlet temperature of the HTF. Hence, a design engineer should consider the datasets, either experimental or numerical, for the FPSC to decide the proper working conditions for the practical application. In the proceeding subsections, an in-depth discussion on the influence of working and design parameters on the outlet temperature and the useful heat are given.

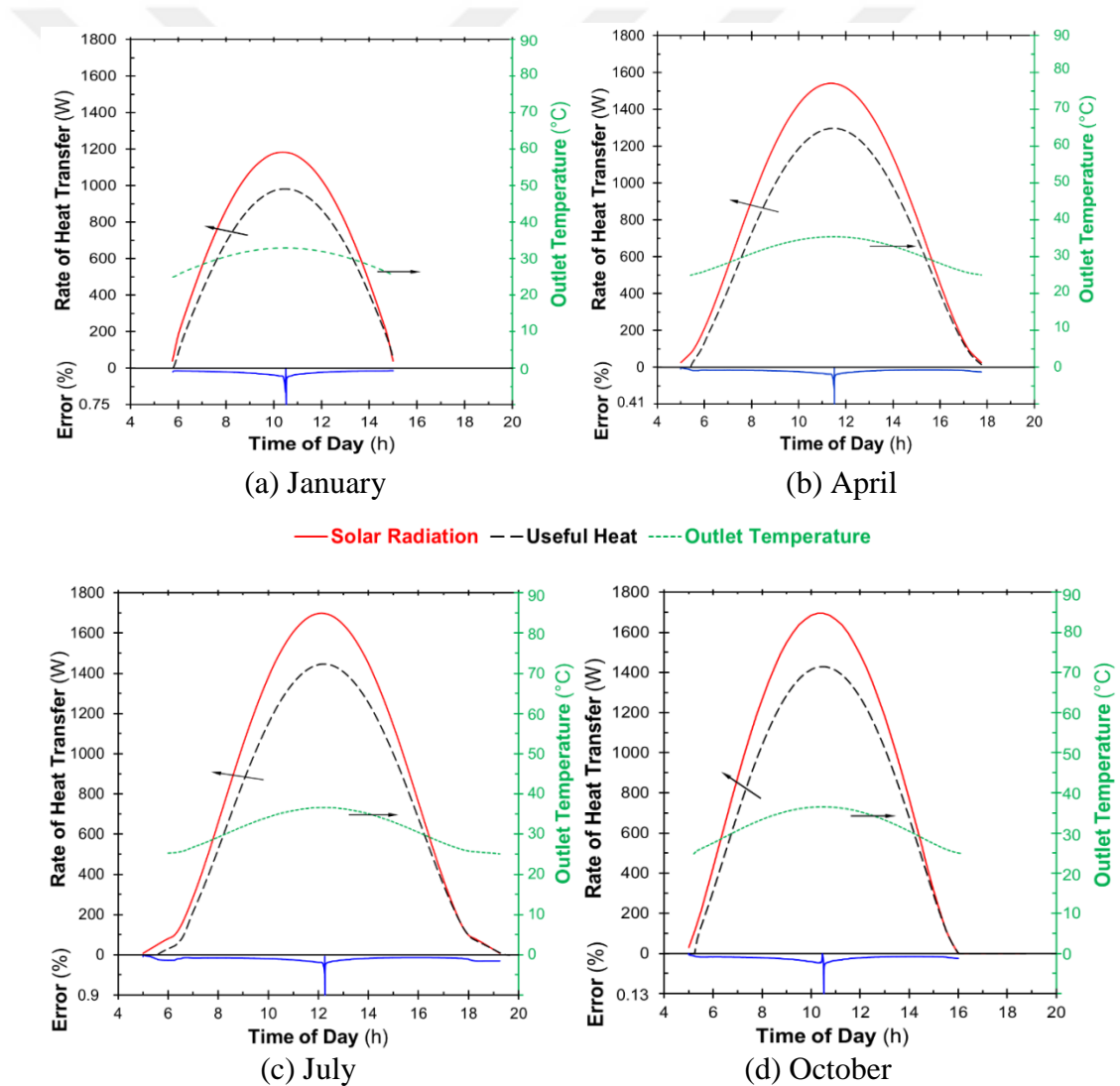


Figure 3.1 Influence of climatic conditions on the FPSC outlet temperature and useful heat for 1% Al<sub>2</sub>O<sub>3</sub>-water nanofluid at 0.03 kg/s

### 3.2. Effect of Working Fluid & Mass Flow Rate on the First Law Efficiency

Figure 3.2 summarizes the influence of the working fluid and the mass flow rate on the performance of an FPSC in October. It is a well-known fact that the thermal resistance between the HTF and the tube wall reduces as the fluid Re number increases. That is, the efficiency increases with increasing mass flow rate regardless of the type of HTF. It is interesting to note that, for lower mass flow rates, such as 0.004 or 0.008 kg/s, the thermal efficiency of the FPSC with ne-HTF is higher than that of pure water. For the flow rates below 0.016 kg/s, increasing the nanoparticle content within the ne-HTF enhances the efficiency. Table 2.3 shows that viscosity of the ne-HTF increases as the nanoparticle content is increased and the specific heat is adversely affected by the nanoparticle loading. Due to nanoparticle addition, the working fluids do not have the same thermophysical properties, so that their critical mass flow rates to enter the turbulence flow regime also differs. While water is turbulent at 0.016 kg/s, ne-HTFs are in laminar condition and have a considerably low convective heat transfer coefficient. Consequently, the efficiency of water increases from 71% to 82% by nearly 10% when the flow regime is changed from laminar to turbulent. On the other hand, ne-HTFs enter the turbulence regime for flow rates higher than 0.016 kg/s. In the turbulent conditions, for the flow rates higher than 0.016 kg/s, it is interesting to note that nanoparticle loading has a negative influence on the efficiency of the FPSC. As stated by Faizal, Saidur, Mekhilef, Hepbasli & Mahbubul (2015), the viscous losses increase at higher flow rates for the nano-enhanced working fluids. Since the pumping power adversely affects the thermal efficiency of the FPSC, at the turbulent flow conditions water becomes the efficient HTF in the current working and design conditions. Even the ne-HTF possess higher thermal conductivity values, the influence of thermal conductivity may lose its impact at higher Reynolds numbers since the convective thermal resistances will reduce significantly comparing the total thermal resistance across the FPSC. For laminar flow, the highest efficiency of nanofluids is obtained as %74.39 at 3% (vol.) and 0.016 kg/s in July. However, the highest efficiency is observed as %83.90 at 1% (vol.) and 0.06 kg/s in October under turbulent flow conditions. The current model is not a steady-state solver; rather it includes the thermal inertia for each component of the FPSC. According to Rodriguez-Hidalgo et al. (2011), the working fluid is responsible for the 30% of the overall thermal inertia.

Consequently, water with a higher specific heat and low viscosity seems to be the most efficient working fluid only at higher flow rates and ne-HTFs are efficient in laminar flow regimes. In Figure 3.3 the thermal efficiencies are given for four selected months and at minimum and maximum flow rates. One can infer that the influences of flow rate and the type of HTF are almost same throughout the year. The use of ne-HTF looks beneficial at lower flow rates regarding the daily average efficiencies.

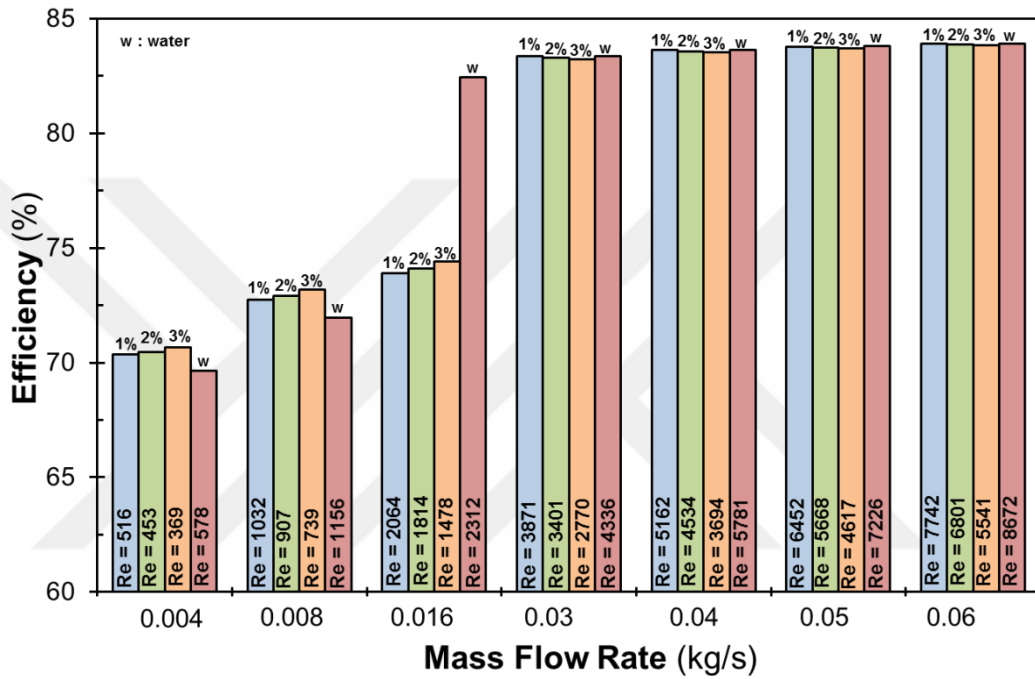


Figure 3.2 Daily average thermal efficiency of the FPSC for various mass flow rates in October

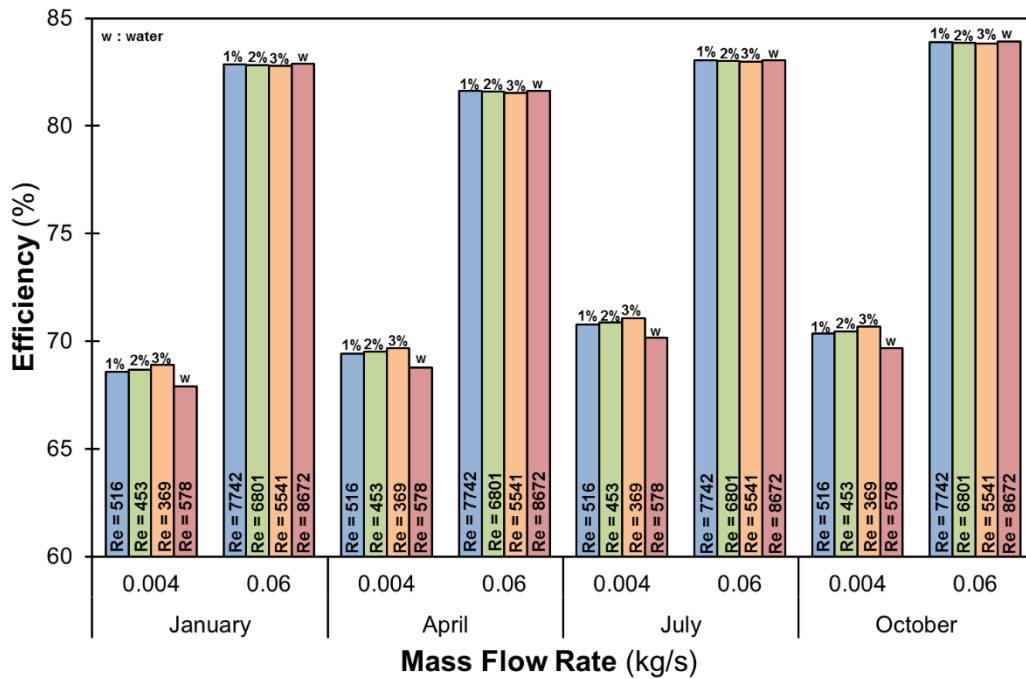


Figure 3.3 Daily average thermal efficiency of the FPSC for various HTFs

In Figures 3.4 and 3.5, the variations of the FPSC efficiencies are illustrated throughout the day by normalizing the time of day into  $(T_{in} - T_{\infty})/I_{solar}$  by following the recent work of Osorio & Carvalho (2014). Curves have similar trends regardless of the working conditions or the type of the HTF. The efficiency of the collector increases as the incident solar radiation increases, which causes a reduction in  $(T_{in} - T_{\infty})/I_{solar}$  parameter. There is an inversion point for each curve that is observed at the minimum  $(T_{in} - T_{\infty})/I_{solar}$  value for the corresponding condition. In Figure 3.4, one can notice that especially for lower flow rates, less than 0.04 kg/s, the efficiency of the collector becomes higher than 100% beyond the inversion point. Such a finding may look unrealistic but considering the thermal inertia effect of the FPSC, the results suit well with the previous observations in the literature (Rodríguez-Hidalgo et al., 2011; Osorio & Carvalho, 2014). The thermal energy that is stored during the daytime is released through the environment and the HTF when the incident solar radiation is below a critical value. Even the insolation is low; there is a great amount of stored energy within the components of the FPSC. At some instants, especially toward sunset, the stored thermal energy which is extracted by the HTF is higher than the incoming solar radiation and the efficiency becomes great than unity. It is also interesting to note that,

the vertical distances between the lower and upper ends of the curves widen as the mass flow rate reduces. This means that at higher flow rates of the HTF, the stored energy inside the FPSC reduces. As mentioned formerly, the working fluid itself is responsible approximately for the 30% of the thermal inertia (Rodríguez-Hidalgo et al., 2011). Hence, at the lower flow rates the fluid domain acts as a sensible storage unit. It stores the solar energy during daytime and releases the stored energy in a very small rate even after sunset. On the contrary, for the higher flow rates, the thermal inertia is very limited. At an arbitrary  $(T_{in} - T_{\infty})/I_{solar}$  value, considering the lower end of the curve, maximum instantaneous efficiency is observed for the higher flow rates. The influence of transition to the turbulence regime is also very sharp in Figure 3.4. At  $(T_{in} - T_{\infty})/I_{solar} = 0.05$  increasing the flow rate from 0.008 to 0.016 kg/s increases the efficiency from 10% to 50%. In Figure 3.5, on the other hand, the influence of ne-HTF on the instantaneous efficiency is given at the maximum and minimum flow rates. Since the curves are overlapping on each other in the wide range of  $(T_{in} - T_{\infty})/I_{solar}$  details for corresponding regions are also given on the plot. Similar to the previous observations, the efficiencies exceed unity. The details for corresponding regions remark an interesting point because the use of ne-HTF does not have the same influence. At lower flow rates, the addition of nanoparticles to the base fluid enhances the efficiency. On the contrary, at higher flow rates the efficiency drops below the base HTF.

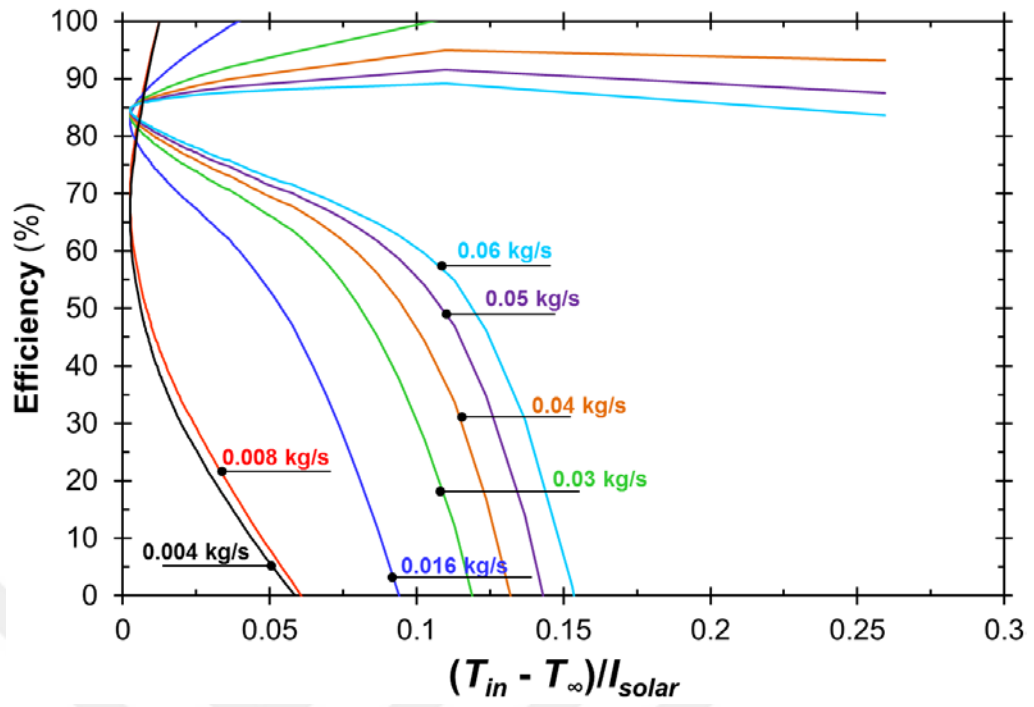


Figure 3.4 Collector efficiency as a function of  $(T_{in} - T_{\infty})/I_{solar}$  parameter for water – Influence of mass flow rate

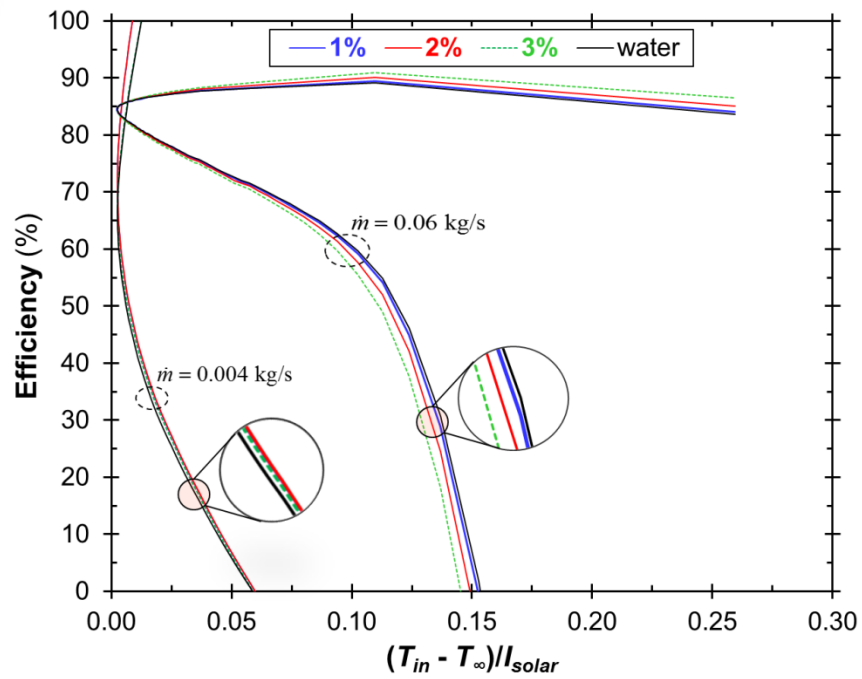
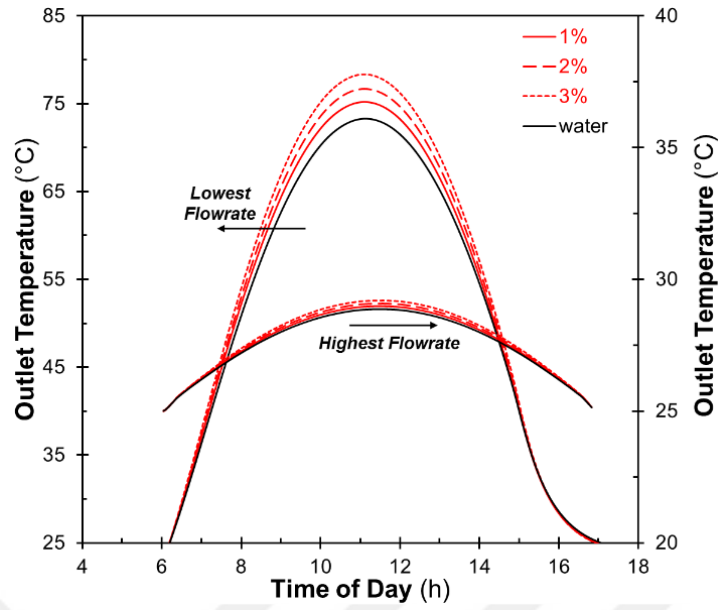


Figure 3.5 Collector efficiency as a function of  $(T_{in} - T_{\infty})/I_{solar}$  parameter – Influence of the type of HTF

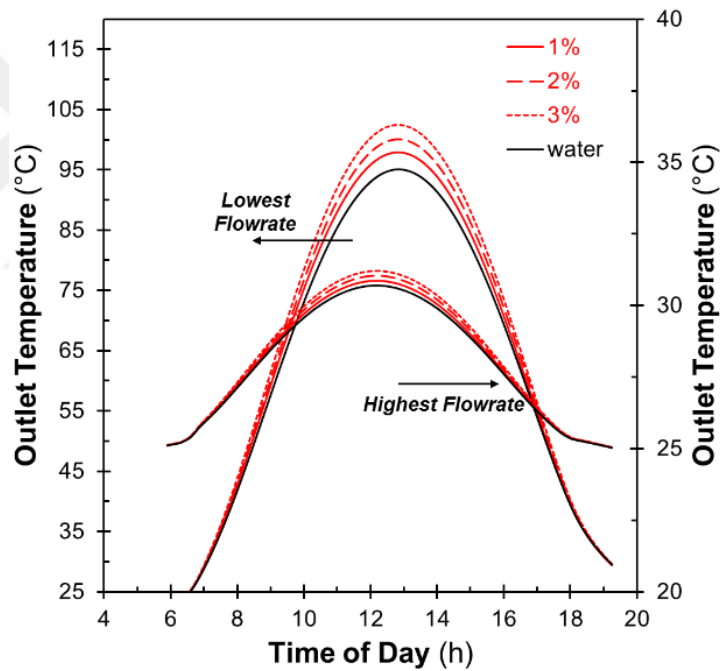
### 3.3. Effect of Working Fluid & Mass Flow Rate on the Outlet Temperature

The influence of mass flow rate of the HTF on the performance of the FPSC is discussed regarding the transient and the mean values of the outlet temperature of the HTF. Figure 3.6 compares the time-wise variation of outlet temperature of the base fluid (*water*) and ne-HTFs with different fractions of nanoparticles. In Figure 3.6 (a) and 3.6 (b) the variations are given for the coldest (*January*) and warmest (*July*) months, respectively. Here the results are given for the lowest and highest flow rate conditions, which correspond to 0.004 and 0.06 kg/s, respectively. For the lowest flow rate, the outlet temperature of the working fluid can reach up to 80°C and 100°C in January and July, respectively. The implementation of the nano-particle shifts the temperature dome upwards. It is certain that increasing the amount of Al<sub>2</sub>O<sub>3</sub> particles within the working fluid raises the outlet temperature in each situation. In January, the maximum temperature of the HTF has been improved by 2.54%, 4.46% and 6.41% as 1%, 2%, and 3% nano-particles are implemented into the base fluid for the lowest flow rate condition. Besides in July, the highest outlet temperature of the HTF has been improved by 2.89%, 5.03% and 7.20% as 1%, 2%, and 3% nano-particles are implemented into the base fluid for the lowest flowrate condition. On the contrary, when the flow rate of the HTF is increased to the highest value, 0.06 kg/s, the temperature dome is flattened. In this working condition, the differences between the outlet temperatures of water based HTF and nano-enhanced HTF with 3% (*vol.*) Al<sub>2</sub>O<sub>3</sub> particles are obtained to be 1.16% and 1.60% for January and July, respectively.





(a)

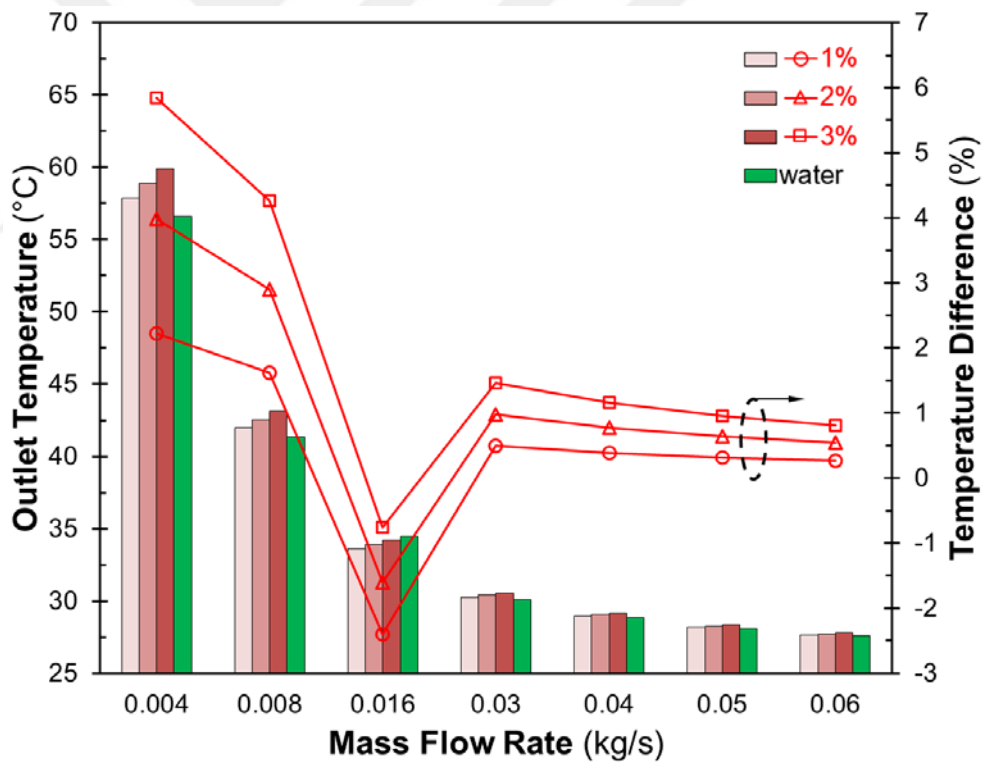


(b)

Figure 3.6 Effect of the mass flow rate of the HTF on the instantaneous outlet temperature for (a) January and (b) July

Figure 3.7 (a) and (b) show the effect of mass flow rate on the average outlet temperature and temperature difference in the coldest, January, and warmest, July, months of the year, respectively. The average outlet temperature decreases with increasing mass flow rates for all working fluids. In the current conditions, the

maximum average temperature is obtained as 64.21°C in July at 3% particle volume concentration and 0.004 kg/s mass flow rate. Moreover, the temperature difference is increased by 6% in July at the same concentration and mass flow rate. At 0.016 kg/s, the addition of nanoparticles inside the base fluid adversely affects the outlet temperature of HTF. Such an observation is consistent with the findings that are explained in detail while discussing Figure 3.1. The variation of the outlet temperature throughout the year is shown in Figure 3.8 regarding the mass flow rate and the type of working fluid. Unlike the efficiency, see Figure 3.1, the outlet temperature of the HTF reduces as the mass flow rate increases and regardless of the laminar or turbulent flow regimes, the nanoparticle has a positive influence on the outlet temperature. The highest outlet temperatures are observed in October. This is due to the selected angle of inclination (45°) and the meteorological data of Izmir City, Turkey.



(a) January

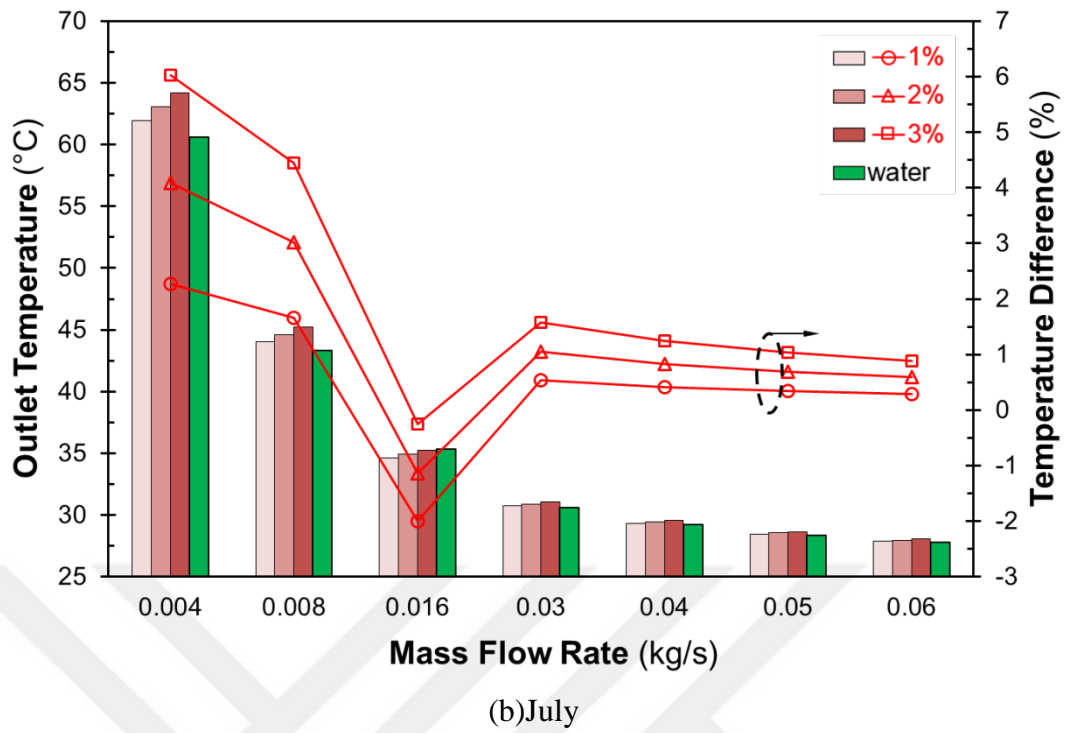


Figure 3.7 The effect of mass flow rates on the average outlet temperature

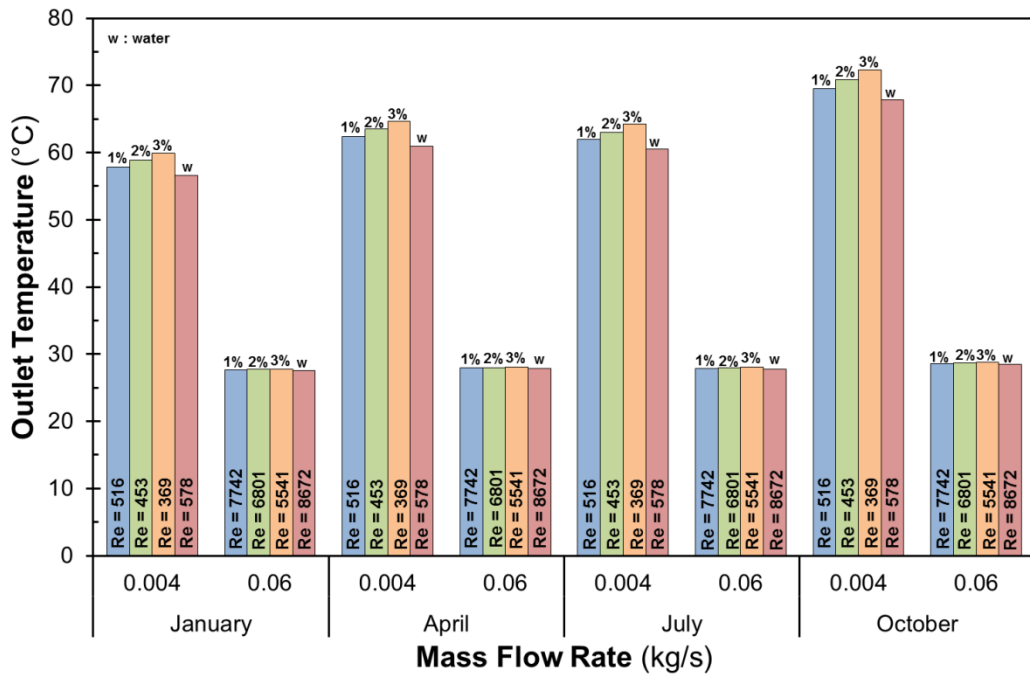


Figure 3.8 Daily average outlet temperature of the FPSC under various HTFs

## CHAPTER FOUR

### CONCLUSION

In this study, the transient behavior of Al<sub>2</sub>O<sub>3</sub>-water nanofluid based FPSC was numerically investigated for different particle volumetric concentrations and mass flow rates at different climatic conditions.

The main conclusions are presented as follows:

- The efficiency of the flat plate solar collector increases with increasing mass flow rates. However, comparison of nanofluid with water gives that nanofluid is more effective on thermal efficiency only at flow rates below 0.016 kg/s whereas, for flow rates water at and above this value, has a higher thermal efficiency. This is due to the flow regime change from laminar to turbulent for water.
- Therefore, there could be a specific flow rate range for enhancing the thermal performance of the systems depending on the thermophysical properties of nanofluids. This dependency should be investigated more systematically.
- Outlet temperature of the working fluids increases with decreasing mass flow rate and increasing volumetric concentration of nanoparticles in the base fluid.
- The maximum increase of outlet temperature was obtained as 7.20% at 0.004 kg/s and 3% (vol.) mass flow rate and volumetric concentration, respectively, in July.
- The average outlet temperature is increased by 6% and the maximum average temperature is obtained as 64.21 °C for 3% (vol.) and 0.004 kg/s mass flow rate, in July.
- For laminar flow, the highest efficiency of nanofluids is obtained as %74.39 at 3% (vol.) and 0.016 kg/s in July. However, the highest efficiency is observed as %83.90 at 1% (vol.) and 0.06 kg/s in October under turbulent flow conditions
- Using transient analyses enables the determination of thermal inertia of each component such as a glass, trapped air, absorber and working fluid which may result in size and cost reduction.

According to aforementioned conclusions, it is observed that nanoparticles are more effective on the outlet temperature of flat plate solar collectors. For the current conditions, nanofluids are promising regarding the thermal efficiency of the system under laminar flow regime. As a future work, transient analysis could be employed for nanofluid based PV/T systems, since the method can provide advantages for parameters such as size and cost in such systems.



## REFERENCES

- Agency, I. E. A. (2016). World Energy Outlook 2016. S.I.: Organization For Economic. Retrieved January 2, 2017, from <https://www.iea.org/publications/freepublications/publication/WorldEnergyOutlook2016ExecutiveSummaryEnglish.pdf>
- Amer, E. H., Nayak, J. K., & Sharma, G. K. (1998). Transient method for testing flat-plate solar collectors. *Energy Conversion and Management*, 39(7), 549-558.
- BP statistical review of world energy June 2016. (2016). BP. Retrieved January 3, 2017, from <https://www.bp.com/content/dam/bp/pdf/energy-economics/statistical-review-2016/bp-statistical-review-of-world-energy-2016-full-report.pdf>
- Cengel, Y. A., Turner, R. H., Cimbala, J. M., & Kanoglu, M. (2005). *Fundamentals of thermal-fluid sciences* (1138). New York, NY: McGraw-Hill.
- Chol, S. U. S. (1995). Enhancing thermal conductivity of fluids with nanoparticles. *ASME-Publications-Fed*, 231, 99-106.
- Colangelo, G., Favale, E., Miglietta, P., de Risi, A., Milanese, M., & Laforgia, D. (2015). Experimental test of an innovative high concentration nanofluid solar collector. *Applied Energy*, 154, 874-881.
- Devendiran, D. K., & Amirtham, V. A. (2016). A review on preparation, characterization, properties and applications of nanofluids. *Renewable and Sustainable Energy Reviews*, 60, 21-40.
- Doganay, S., & Turgut, A. (2015). Enhanced effectiveness of nanofluid based natural circulation mini loop. *Applied Thermal Engineering*, 75, 669-676.

- Duffie, J.A. & Beckman, W.A. (1974). *Solar energy thermal process*. New York: Wiley Interscience.
- Eastman, J. A., Phillpot, S. R., Choi, S. U. S., & Keblinski, P. (2004). Thermal transport in nanofluids 1. *Annu. Rev. Mater. Res.*, *34*, 219-246.
- Ekramian, E., Etemad, S. G., & Haghshenasfard, M. (2014). Numerical Investigations of Heat Transfer Performance of Nanofluids in a Flat Plate Solar Collector. *Journal ISSN*, *1929*, 1248.
- Energy and Economics; The Institute of Energy Economics, JAPAN. (2016). Retrieved September 26, 2017, from [https://www.ief.org/\\_resources/files/snippets/ieej/ieej\\_outlook2016\\_\\_7007\\_rv\\_for\\_ief.pdf](https://www.ief.org/_resources/files/snippets/ieej/ieej_outlook2016__7007_rv_for_ief.pdf)
- Faizal, M., Saidur, R., Mekhilef, S., & Alim, M. A. (2013). Energy, economic and environmental analysis of metal oxides nanofluid for flat-plate solar collector. *Energy Conversion and Management*, *76*, 162-168.
- Faizal, M., Saidur, R., Mekhilef, S., Hepbasli, A., & Mahbubul, I. M. (2015). Energy, economic, and environmental analysis of a flat-plate solar collector operated with SiO<sub>2</sub> nanofluid. *Clean Technologies and Environmental Policy*, *17*(6), 1457-1473.
- Fernandes, M. S., Brites, G. J. V. N., Costa, J. J., Gaspar, A. R., & Costa, V. A. F. (2016). A thermal energy storage system provided with an adsorption module—Dynamic modeling and viability study. *Energy Conversion and Management*, *126*, 548-560.
- Ganvir, R. B., Walke, P. V., & Kriplani, V. M. (2016). Heat transfer characteristics in nanofluid—A review. *Renewable and Sustainable Energy Reviews*.

- Hamed, M., Fellah, A., & Brahim, A. B. (2014). Parametric sensitivity studies on the performance of a flat plate solar collector in transient behavior. *Energy Conversion and Management*, 78, 938-947.
- Hussein, A. K. (2016). Applications of nanotechnology to improve the performance of solar collectors—Recent advances and overview. *Renewable and Sustainable Energy Reviews*, 62, 767-792.
- Incropera, FP. Dewitt, DP. Bergman TL, & Lavine VS. (2006). *Fundamentals of heat and mass transfer*. 6th ed.
- International Energy Outlook 2017 (IEO2017). Retrieved September 26, 2017, from [https://www.eia.gov/outlooks/aeo/pdf/0383\(2017\).pdf](https://www.eia.gov/outlooks/aeo/pdf/0383(2017).pdf).
- Kalogirou, S. A. (2004). Solar thermal collectors and applications. *Progress in energy and combustion science*, 30(3), 231-295.
- Kong, W., Wang, Z., Fan, J., Bacher, P., Perers, B., Chen, Z., & Furbo, S. (2012). An improved dynamic test method for solar collectors. *Solar Energy*, 86(6), 1838-1848.
- Leong, K. Y., Ong, H. C., Amer, N. H., Norazrina, M. J., Risby, M. S., & Ahmad, K. K. (2016). An overview on current application of nanofluids in solar thermal collector and its challenges. *Renewable and Sustainable Energy Reviews*, 53, 1092-1105.
- Masuda, H., Ebata, A., & Teramae, K. (1993). Alteration of thermal conductivity and viscosity of liquid by dispersing ultra-fine particles. Dispersion of Al<sub>2</sub>O<sub>3</sub>, SiO<sub>2</sub> and TiO<sub>2</sub> ultra-fine particles. *Netsu Bussei*, 7, 227-233.



- Moghadam, A. J., Farzane-Gord, M., Sajadi, M., & Hoseyn-Zadeh, M. (2014). Effects of CuO/water nanofluid on the efficiency of a flat-plate solar collector. *Experimental Thermal and Fluid Science*, 58, 9-14.
- Nasrin, R., & Alim, M. A. (2014a). Finite element simulation of forced convection in a flat plate solar collector: Influence of nanofluid with double nanoparticles. *Journal of Applied Fluid Mechanics*, 7(3), 543-556.
- Nasrin, R., & Alim, M. A. (2014b). Semi-empirical relation for forced convective analysis through a solar collector. *Solar Energy*, 105, 455-467.
- Nayak, J. K., Amer, E. H., & Deshpande, S. M. (2000). Comparison of three transient methods for testing solar flat-plate collectors. *Energy conversion and management*, 41(7), 677-700.
- Onyegebu, S. O., & Morhenne, J. (1993). Transient multidimensional second law analysis of solar collectors subjected to time-varying insolation with diffuse components. *Solar energy*, 50(1), 85-95.
- Osório, T., & Carvalho, M. J. (2014). Testing of solar thermal collectors under transient conditions. *Solar Energy*, 104, 71-81.
- Panayiotou, G. P., Kalogirou, S. A., Florides, G. A., Roditis, G., Katsellis, N., Constantinou, A., ... & Nielsen, J. E. (2016). Experimental Investigation of the Effect of Solar Collector's Inclination Angle on the Generation of Thermosiphonic Flow. In *Renewable Energy in the Service of Mankind Vol II* (807-816). *Springer International Publishing*.
- Pandey, K. M., & Chaurasiya, R. (2017). A review on analysis and development of solar flat plate collector. *Renewable and Sustainable Energy Reviews*, 67, 641-650.
- Patankar, S. (1980). *Numerical heat transfer and fluid flow*. CRC Press.

- Photovoltaic Geographical Information System - Interactive Maps (2017). Retrieved June 24, 2016, from <http://re.jrc.ec.europa.eu/pvgis/apps4/pvest.php>
- Raja, M., Vijayan, R., Dineshkumar, P., & Venkatesan, M. (2016). Review on nanofluids characterization, heat transfer characteristics and applications. *Renewable and Sustainable Energy Reviews*, *64*, 163-173.
- Rodríguez-Hidalgo, M. C., Rodríguez-Aumente, P. A., Lecuona, A., Gutiérrez-Urueta, G. L., & Ventas, R. (2011). Flat plate thermal solar collector efficiency: Transient behavior under working conditions. Part I: Model description and experimental validation. *Applied Thermal Engineering*, *31*(14), 2394-2404.
- Sarsam, W. S., Kazi, S. N., & Badarudin, A. (2015). A review of studies on using nanofluids in flat-plate solar collectors. *Solar Energy*, *122*, 1245-1265.
- Suman, S., Khan, M. K., & Pathak, M. (2015). Performance enhancement of solar collectors—A review. *Renewable and Sustainable Energy Reviews*, *49*, 192-210.
- Swinbank, W. C. (1963). Long-wave radiation from clear skies. *Quarterly Journal of the Royal Meteorological Society*, *89*(381), 339-348.
- T.C. Orman ve Su İşleri Bakanlığı Meteoroloji Genel Müdürlüğü Meteoroloji 2. Bölge Müdürlüğü (2017). Retrieved June 24, 2016, from [http://www.izmir.mgm.gov.tr/files/iklim/izmir\\_iklim.pdf/](http://www.izmir.mgm.gov.tr/files/iklim/izmir_iklim.pdf/)
- Tora, E. A. H., & Moustafa, T. (2013). Numerical Simulation of an Al<sub>2</sub>O<sub>3</sub>-H<sub>2</sub>O Nanofluid as a Heat Transfer Agent for a Flat-Plate Solar Collector. *International Journal of Scientific & Engineering Research*, *4*(5), 562-573.

- Turgut, A., & Doganay, S. (2014). Thermal performance of a single phase natural circulation mini loop working with nanofluid. *High Temperatures--High Pressures*, 43(4).
- Turgut, A., Saglanmak, S., & Doganay, S. (2016). Experimental Investigation on Thermal Conductivity and Viscosity of Nanofluids: Particle Size Effect. *Journal of The Faculty of Engineering and Architecture of Gazi University*, 31(1), 95-103.
- UNFCCC. Adoption of the Paris Agreement. Report No. FCCC/CP/2015/L.9/Rev.1. Retrieved January 2, 2016, from <http://unfccc.int/resource/docs/2015/cop21/eng/l09r01.pdf> (UNFCCC, 2015)
- Verma, S. K., & Tiwari, A. K. (2015). Progress of nanofluid application in solar collectors: a review. *Energy Conversion and Management*, 100, 324-346.
- Verma, S. K., Tiwari, A. K., & Chauhan, D. S. (2016). Performance augmentation in flat plate solar collector using MgO/water nanofluid. *Energy Conversion and Management*, 124, 607-617.
- Verma, S. K., Tiwari, A. K., & Chauhan, D. S. (2017). Experimental evaluation of flat plate solar collector using nanofluids. *Energy Conversion and Management*, 134, 103-115.
- Vincely, D. A., & Natarajan, E. (2016). Experimental investigation of the solar FPC performance using graphene oxide nanofluid under forced circulation. *Energy Conversion and Management*, 117, 1-11.
- Yousefi, T., Veisy, F., Shojaeizadeh, E., & Zinadini, S. (2012). An experimental investigation on the effect of MWCNT-H<sub>2</sub>O nanofluid on the efficiency of flat-plate solar collectors. *Experimental Thermal and Fluid Science*, 39, 207-212.

## APPENDICES

### Abbreviations

$A$	area ( $\text{m}^2$ )
$c$	specific heat ( $\text{J/kgK}$ )
$f$	Darcy friction factor
$g$	gravitational acceleration ( $\text{m/s}^2$ )
$Gr$	Grashof number ( $= g\beta\Delta TL_c^3/\nu^2$ )
$h$	convective heat transfer coefficient ( $\text{W/m}^2\text{K}$ )
$I_{solar}$	incident solar radiation ( $\text{W/m}^2$ )
$i, j$	node number in 2D space
$k$	thermal conductivity ( $\text{W/mK}$ )
$L$	length of the tube
$L_c$	characteristic length (m)
$m$	mass (kg)
$\dot{m}$	mass flow rate ( $\text{kg/s}$ )
$Nu$	Nusselt number ( $= hL_c/k$ )
$P$	pressure (Pa)
$Pr$	Prandtl number ( $= \mu c/k$ )
$Re$	Reynolds number ( $= \rho VD/\mu$ )
$q$	rate of heat transfer (W)
$t$	time (s)
$T$	Temperature (K or $^{\circ}\text{C}$ )
$V$	velocity (m/s)
$v_{wind}$	wind speed (m/s)
$\dot{W}$	pumping power (W)
$x, y$	position in Cartesian coordinates (m)
FPSC	Flat plate solar collector
HTF	Heat transfer fluid
ne-HTF	Nano-enhanced heat transfer fluid
TES	Thermal energy storage

### ***Subscripts***

<i>abs</i>	absorber
<i>f</i>	fluid
<i>g</i>	glass
<i>htf</i>	heat transfer fluid
<i>in</i>	inlet
<i>c</i>	cross section
<i>out</i>	outlet
<i>p</i>	particle
<i>s</i>	surface

### ***Greek Letters***

$\alpha$	absorptivity
$\beta$	thermal expansion coefficient (1/K)
$\varepsilon$	emissivity
$\eta$	efficiency
$\theta$	angle of inclination
$\mu$	dynamic viscosity (Pas)
$\rho$	density (kg/m <sup>3</sup> )
$\sigma$	Stefan-Boltzmann constant (= 5.67x10 <sup>-8</sup> W/m <sup>2</sup> K <sup>4</sup> )
$\tau$	transmissivity
$\vartheta$	kinematic viscosity (m <sup>2</sup> /s)
$\phi$	particle volume fraction